ELSEVIER

Journal of Photochemistry and Photobiology A: Chemistry 108 (1997) 159–167

Journal of PHOTOCHEMISTRY AND PHOTOBIOLOGY A: CHEMISTRY

EPR studies of the photodynamic action of mercapto-substituted hypocrellin B derivatives: formation of semiquinone radical anion and activated oxygen on illumination with visible light

Min Weng, Manhua Zhang *, Tao Shen

Institute of Photographic Chemistry, Academia Sinica, Beijing 100101, People's Republic of China

Received 1 November 1996; revised 14 January 1997; accepted 30 January 1997

Abstract

Perylenequinonoid pigments exhibit several photodynamic therapeutic advantages over the commonly used haematoporphyrin derivatives. Two types of mercapto-substituted hypocrellin B derivatives (5,8-RS-HB, 5-RS-HB) were prepared. The photophysical and photochemical properties of the mercapto-substituted hypocrellin B derivatives were investigated. When 5,8-RS-HB or 5-RS-HB was illuminated with visible light, semiquinone radical anion, superoxide anion radical, singlet oxygen and hydroxyl radical were detected. The formation of semiquinone radical anion and activated oxygen and the transformation and competition between them depend on the sample and oxygen concentrations, the time and intensity of illumination and the nature of the substrate. In anaerobic solution, the semiquinone radical anion was predominantly photoproduced via the self-electron transfer between the excited and ground species. In aerobic solution, singlet oxygen was generated. In addition, the superoxide anion radical was also generated by 5,8-RS-HB or 5-RS-HB on illumination in aerobic solution. The superoxide anion radical was produced via the reduction of oxygen by the semiquinone radical anion, and this process was significantly enhanced by the presence of electron donors. In DMSO–H_2O (1 : 1, v/v) solution, the hydroxyl radical was observed via the Fenton reaction. On the basis of these results, both electron transfer (type I) and $^1O_2$ (type II) paths were found to be involved in 5,8-RS-HB and 5-RS-HB photosensitization to different extents. © 1997 Elsevier Science S.A.

Keywords: EPR; Photodynamic action; Photosensitization; Reactive oxygen species; Semiquinone radical anion

1. Introduction

Hypocrellin A and B (HA and HB) (Fig. 1) have recently been isolated from natural fungus sacs of *Hypocrella bambusae* in China. These lipid-soluble 4,9-dihydroxy-3,10-perylenequinone derivatives, employed in pioneering photodynamic therapy (PDT) applications of perylenequinonoid pigments (PQPS) [1,2], exhibit several advantages over the presently used haematoporphyrin derivatives (HPD), i.e. easy preparation and purification relative to HPD, small aggregation tendency (which decreases the efficiency of HPD), strong red light absorptivity and significantly reduced normal tissue photosensitivity because of the fast metabolism in vivo [3]. As a result, hypocrellins have been successfully employed in the clinical PDT treatment of a number of skin diseases, such as white lesions of vulva, keloid, vitiligo, psoriasis, tinea capitis and lichen amyloidosis [4–6] without the observation of the prolonged normal tissue photosensitivity

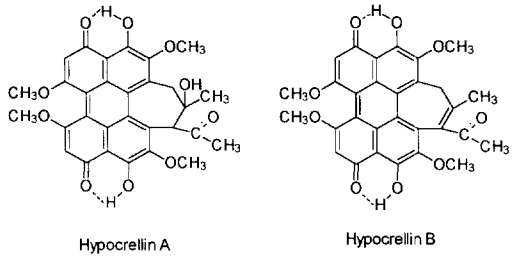

Fig. 1. Chemical structures of hypocrellin A and hypocrellin B.

which occurs with HPD [3]. It has also been shown that hypocrellins are efficient singlet oxygen generators [7], and demonstrate some advantages over the classic $^1O_2$ sensitizers (such as porphyrins, rose bengal, methylene blue, etc.), including high molar extinction coefficients, wide UV–visible absorption, high quantum yields of singlet oxygen generation, high stability, good solubility and small solvent and concentration effects [8].

The latest studies have indicated that the target of photodynamic action of hypocrellin is the cell membrane, this

* Corresponding author.

PII S1010-6030(97)00072-5

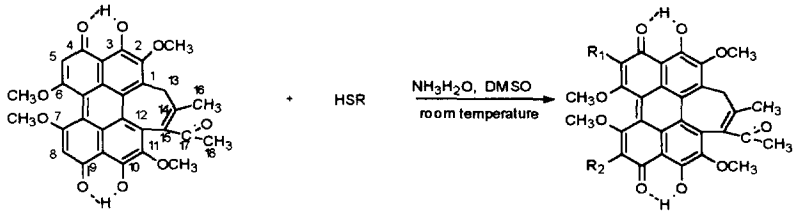

$R=(CH_2)_{11}CH_3$

5-RS-HB:R1=$S(CH_2)_{11}CH_3$ R2=H

5,8-RS-HB:R1=R2=$S(CH_2)_{11}CH_3$

Scheme 1.

photodynamic action causing an evident reduction in the quantity of mercapto groups in membrane proteins. Until recently, relatively little effort has been devoted to the study of the mechanism of this photodynamic action. This has encouraged us to study the reaction of HB with mercapto compounds and the photodynamic action of mercapto-substituted HB derivatives.

In this work, two types of mercapto-substituted HB derivatives (5,8-RS-HB, 5-RS-HB) (Scheme 1) were successfully synthesized in high yield and characterized. When 5,8-RS-HB or 5-RS-HB was illuminated with visible light, the formation process of semiquinone radical anion and activated oxygen ($^1O_2$, $O_2^{\cdot-}$, $^{\cdot}OH$) was studied by electron paramagnetic resonance (EPR) in detail. The formation mechanism of superoxide radical anion and the effect of oxygen on the competition between type I and II mechanisms of photosensitization are also reported.

2. Materials and methods

2.1. Materials

HA and HB were extracted from fungus sacs of *Hypocrella bambusae* and purified by recrystallization from acetone. 5,5-Dimethyl-1-pyrroline-*N*-oxide (DMPO) and 9,10-diphenylanthracene (9,10-DPA) were obtained from Aldrich Chemical Company. 2,2,6,6-Tetramethyl-4-piperidone (TEMP) was purchased from Merck Chemical Company. Superoxide dismutase (SOD) and cysteine were purchased from Biotech Technology Corporation, Chinese Academy of Sciences. Diethylaniline, *N*-ethylaniline, aniline, sodium azide, dodecyl mercaptan, dimethylsulphoxide (DMSO) and other solvents, all of analytical grade, were purchased from Beijing Chemical Plant. Water was freshly distilled before use. The solutions were purged with oxygen, air or argon according to experimental requirements. The required high-purity solvents were prepared by further purification of the commercial products, and no impurities were detected by absorption and/or fluorescence spectroscopy. Absorption spectra were recorded with a Shimadzu UV-160A UV–visible spectrophotometer. The samples were bubbled with highly purified argon for 30 min and irradiated with a 450 W medium-pressure sodium lamp before measurement. Fluorescence spectra were measured with a Hitachi MPF-4 fluorometer. Proton nuclear magnetic resonance (^1H-NMR) spectra were measured with a Varian XL-400. Mass spectra were performed by a ZAB-HS (fast atom bombardment mass spectrometer).

2.2. Preparation of 5,8-RS-HB and 5-RS-HB

HB (40 mg) was dissolved in DMSO (40 ml), and 28% ammonium hydroxide was added to adjust the pH (9–10); dodecyl mercaptan (2 ml) was then added in the dark under argon. The resulting solution was stirred in the dark for 3 h at room temperature, and the mixture was poured into ice–water, neutralized with 10% hydrochloric acid and extracted with chloroform three to four times. The chloroform layer was washed with water three times. The solvent chloroform was evaporated under reduced pressure to obtain a violet red solid. The solid was purified by thin layer chromatography (TLC) on a 1% citric acid–silica gel plate using 4 : 2 : 1 (v/v/v) petroleum ether–ethyl acetate–ethanol, and the compounds 5,8-RS-HB (42 mg; yield, 60%) and 5-RS-HB (17 mg; yield, 30%) were obtained.

5-RS-HB. IR: 3350, 1692 and 1601 cm^{-1}. ^1H-NMR: 15.97 (s, 1H, exchanged with D_2O, 4(9)-OH), 15.94 (s, 1H, exchanged with D_2O, 9(4)-OH), 6.42 (s, 1H, 5(8)-H), 2.38 (s, 3H, 18-CH_3), 1.97 (s, 3H, 16-CH_3), 4.02 (s, 3H, 6-OCH_3), 4.14 (s, 3H, 2-OCH_3), 4.07 (s, 3H, 7-OCH_3), 4.10 (s, 3H, 11-OCH_3), 4.04 (d, 1H, 13-H_2, $J=11.8$ Hz), 3.23 (d, 1H, 13-H_2, $J=11.8$ Hz), 3.61–3.81 (m, 4H, -SCH_2CH_2), 1.61 (m, 18H, CH_2-), 1.22 (t, 3H, -$SRCH_3$). MS (*m/z*) (FAB): 728 (M^+).

5,8-RS-HB. IR: 3348, 1694 and 1601 cm^{-1}. ^1H-NMR: 15.98 (s, 1H, exchanged with D_2O, 4(9)-OH), 15.95 (s, 1H, exchanged with D_2O, 9(4)-OH), 2.38 (s, 3H, 18-CH_3), 1.96 (s, 3H, 16-CH_3), 3.88 (s, 3H, 6-OCH_3), 4.15 (s, 3H, 2-OCH_3), 3.92 (s, 3H, 7-OCH_3), 4.08 (s, 3H, 11-OCH_3), 4.04 (d, 1H, 13-H_2, $J=11.8$ Hz), 3.25 (d, 1H, 13-H_2, $J=11.8$ Hz), 3.09–3.345 (m, 8H, -SCH_2CH_2), 1.30–1.68 (m, 36H, CH_2-), 1.21 (t, 6H, -$SRCH_3$); MS (*m/z*) (FAB): 928 (M^+).

2.3. Spin trapping and EPR measurements

The superoxide radical anion ($O_2^{\cdot-}$) and hydroxyl radicals ($^{\cdot}OH$) produced were identified by means of the spin trapping method with EPR detection. Measurements of the EPR spectra were carried out on a Bruker ER-300 EPR spectrometer operating at room temperature (X band; microwave frequency, 9.5 GHz). Samples (25 μl) were injected quantitatively into specially made quartz capillaries for EPR analysis and were illuminated with a 450 W medium-pressure sodium lamp. A long pass filter was employed to eliminate light at wavelengths of less than 470 nm.

2.4. Quantum yield of $^1O_2$ generation

The quantum yields of $^1O_2$ generation of HB, 5,8-RS-HB and 5-RS-HB were determined using the 9,10-DPA bleaching method established by Diwu and Lown [8]. The reactions were followed spectrophotometrically by observing the decrease in the 374 nm absorption peak of 9,10-DPA (where the sensitizers used have the lowest absorptivity) as a function of the irradiation time. The photo-oxidations of DPA sensitized by HB, 5,8-RS-HB and 5-RS-HB were carried out on a "merry-go-round", where the sample was illuminated by 579 nm light, obtained from the combination of a medium-pressure sodium lamp with a narrow band interference filter. The spin trapping of $^1O_2$ by TEMP was used as an alternative method to determine the formation of $^1O_2$ by HB, 5,8-RS-HB or 5-RS-HB. The spin trapping of $^1O_2$ by TEMP was performed according to a modification of Lion's method. Typically, the reaction solution consisted of 3.4×10^{-5} M of sample and 10 mM of TEMP. These two methods gave consistent results.

3. Results and discussion

3.1. EPR measurements of free radicals produced during the photosensitization of mercapto-substituted HB derivatives

Illumination of 5,8-RS-HB (1 mM) or 5-RS-HB (1 mM) in an argon-gassed DMSO solution for 2 min leads to the generation of the strong EPR signal shown in Fig. 2. The intensity of the EPR signal increases rapidly during photoirradiation and decreases very slowly in the dark. When the sample is exposed to oxygen, the EPR signal is quenched (Fig. 2(D)). The EPR signal intensities of the 5,8-RS-HB and 5-RS-HB radicals also depend on the concentration of the sample, the illumination time and intensity. The concentrations of 5,8-RS-HB and 5-RS-HB exert such a strong effect on the generation of the radicals that the signals of the 5,8-RS-HB and 5-RS-HB radicals can be observed even in aerated DMSO at high concentration. In a previous report, Hu et al. [9] demonstrated that the HA radical may be generated by self-electron transfer between the ground and excited species. It is believed that a similar mechanism is involved in the generation of 5,8-RS-HB and 5-RS-HB radicals

$$5,8-RS-HB^* + 5,8-RS-HB \rightarrow 5,8-RS-HB^{\cdot-} + 5,8-RS-HB^{\cdot+} \quad (1)$$

In general, the radical cation of quinone is difficult to detect in common organic solvents owing to its strong oxidizing ability [10]; thus the EPR spectrum observed may be ascribed to the semiquinone radical anions of 5,8-RS-HB and 5-RS-HB. In order to identify the EPR signal shown in Fig. 2, the following experiments were performed.

1. 5,8-RS-HB (1 mM) or 5-RS-HB (1 mM) in DMSO was illuminated in the presence of *N,N*-diethylaniline (DEA), a typical reductant ($E_0(D^+/D) = 0.34$ V), for 1 min. The EPR spectrum (Fig. 2(C)) obtained is very similar to that observed in the absence of DEA. From Fig. 2(D), it can also be seen that the addition of DEA intensifies the EPR signal significantly. This indicates the anionic character of the 5,8-RS-HB and 5-RS-HB radicals. A series of other electron donors, including *N*-ethylaniline, aniline, cysteine, ascorbate and ethylenediaminetetraacetic acid (EDTA), were used instead of DEA and similar results were obtained. These reduced substrates, more electron-rich than 5,8-RS-HB or 5-RS-HB, may donate an electron directly to excited 5,8-RS-HB or 5-RS-HB. In the pres-

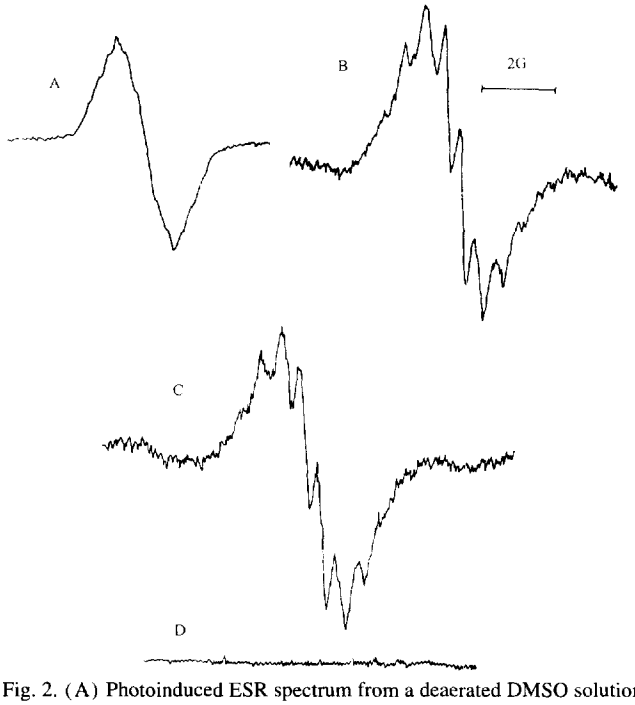

Fig. 2. (A) Photoinduced ESR spectrum from a deaerated DMSO solution of 5,8-RS-HB (1 mM) irradiated above 470 nm for 2 min. (B) Same as (A), but the photosensitizer is 5-RS-HB (1 mM). (C) Same as (A), but in the presence of DEA (5 mM) and irradiation for 30 s. (D) Same as (A), but oxygen was bubbled through the solution after illumination. Instrumental settings (spectra A, B and D): microwave power, 1.01 mW; modulation amplitude, 0.166 G; scan range, 20 G; receiver gain, 2×10^5. Instrumental settings (spectrum C): microwave power, 1.01 mW; modulation amplitude, 0.166 G; scan range, 20 G; receiver gain, 2×10^4.

ence of electron donor (D), 5,8-RS-HB$^{\bullet -}$ and 5-RS-HB$^{\bullet -}$ may be generated by

$$5,8-RS-HB^{*}+D \rightarrow 5,8-RS-HB^{\bullet -}+D^{+} \quad (2)$$

2. The EPR signals of the 5,8-RS-HB and 5-RS-HB radicals are quenched significantly by oxygen, the EPR signal disappearing completely when oxygen is bubbled through solutions of 5,8-RS-HB and 5-RS-HB radicals. Furthermore, when DMPO and oxygen are present in solutions of 5,8-RS-HB and 5-RS-HB radicals, the EPR signal of the DMPO–superoxide radical adduct is detected immediately, accompanied by the disappearance of the EPR signals of the 5,8-RS-HB and 5-RS-HB radicals (details discussed below).
3. The kinetics of decay of the radical were measured by recording the decrease in the amplitude of the EPR signal from its steady state level after illumination was stopped (Fig. 3). The results show that the 5,8-RS-HB and 5-RS-HB radicals decay according to second-order kinetics. In accordance with these results, the observed EPR spectrum is considered to originate from 5,8-RS-HB$^{\bullet -}$ and 5-RS-HB$^{\bullet -}$.

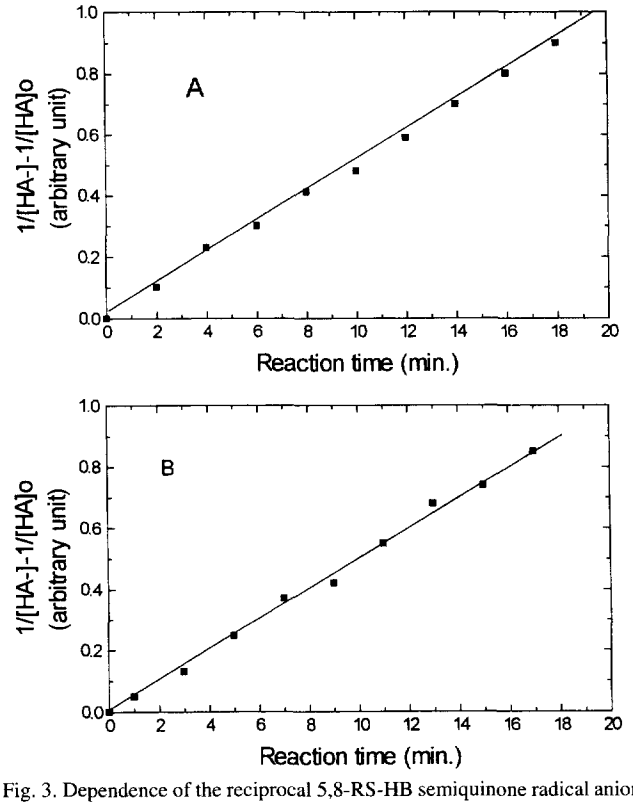

Fig. 3. Dependence of the reciprocal 5,8-RS-HB semiquinone radical anion concentration on the time of dark reaction in DMSO. (A) Measured from the decay of the amplitude of the EPR signal of 5,8-RS-HB$^{\bullet -}$. (B) Measured from the decay of the optical density of 5,8-RS-HB$^{\bullet -}$ at 655 nm. 5,8-RS-HB$^{\bullet -}$ was generated by illumination of an argon-gassed DMSO solution of 5,8-RS-HB and DEA.

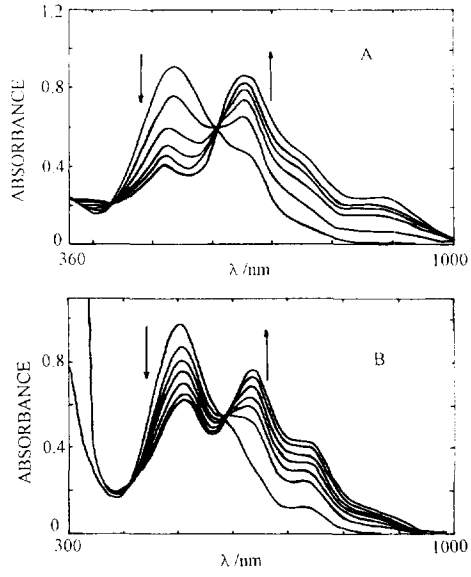

Fig. 4. Absorption spectral changes observed on irradiation. Photoreduction of 5,8-RS-HB (A) and 5-RS-HB (B) (5×10^{-5} mol l^{-1}) by DEA (5×10^{-3} mol l^{-1}) in deaerated DMSO. Arrows indicate the direction of the changes.

3.2. *Spectrophotometric measurements of deoxygenated solutions of 5,8-RS-HB/5-RS-HB and electron donor*

The UV–visible absorption spectra of 5,8-RS-HB and 5-RS-HB are shown in Fig. 4. The addition of electron donor (DEA) does not affect the absorption spectra of 5,8-RS-HB and 5-RS-HB, indicating the absence of ground state interaction between 5,8-RS-HB/5-RS-HB and DEA. When 5,8-RS-HB in a deaerated solution of DMSO is irradiated in the presence of DEA, the colour of the sample changes from purple to green; the absorbance of 5,8-RS-HB at 535 nm continuously decreases, while the 655 nm absorbance increases generating an isosbestic point at 608 nm. The presence of the isosbestic point at 608 nm shows that only two species, i.e. 5,8-RS-HB and its photoreduced product, exist. We suggest that the photoreduced product of 5,8-RS-HB is 5-RS-HB$^{\bullet -}$ and the absorption at 655 nm can be attributed to 5,8-RS-HB$^{\bullet -}$ for the following reasons:

1. the product is formed in the presence of a reductant on irradiation and deaeration; when air is caused to re-enter the photoreduction system, the product reverts quantitatively to 5,8-RS-HB;
2. the decay constant of the absorption at 655 nm and the EPR signal of 5,8-RS-HB$^{\bullet -}$ are consistent in the dark.

An analogous result for 5-RS-HB was also obtained in DMSO (Fig. 4).

Thus 5,8-RS-HB$^{\bullet -}$ and 5-RS-HB$^{\bullet -}$ may be responsible for type I photosensitization of 5,8-RS-HB and 5-RS-HB under hypoxic conditions. The photoinduced EPR spectra of 5,8-RS-HB$^{\bullet -}$ and 5-RS-HB$^{\bullet -}$ disappear when oxygen is bubbled through the sample. This observation suggests that oxidation of the semiquinone radical anion by dissolved oxygen occurs. This reaction should produce superoxide anion radi-

cal, and subsequent experiments were carried out in order to examine this possibility.

3.3. Formation of superoxide radical anion

It has been demonstrated that $O_2^{\bullet-}$ is implicated in the photosensitization of amino-substituted hypocrellin derivatives [11]. Here 5,8-RS-HB was used as a representative structure to investigate the generation of $O_2^{\bullet-}$. DMPO spin trapping has been successfully applied to trap certain reactive radical intermediates, in particular $O_2^{\bullet-}$ and hydroxyl radical, because it has a high affinity for reactive radicals and leads to the formation of persistent spin adducts. The EPR spectra of the spin adducts exhibit a primary ^{14}N triplet which is split into a secondary doublet due to coupling with the β-proton of DMPO.

When an oxygen-saturated DMSO solution of 5,8-RS-HB (0.1 mM) and DMPO (30 mM) is irradiated at wavelengths above 470 nm, a multiplet EPR spectrum appears (Fig. 5). This EPR spectrum is characterized by three coupling constants, which are due to the presence of the nitrogen atom and two hydrogen atoms in the β and γ positions. The hyperfine coupling constants ($a^N = 12.7$ G, $a_\beta^H = 10.3$ G, $a_\gamma^H = 1.5$ G) determined for this EPR spectrum (Fig. 5) are consistent with previously reported values for the DMPO–$O_2^{\bullet-}$ radical adduct in DMSO [12]. In the absence of light, oxygen or 5,8-RS-HB, no detectable EPR signal is observed, indicating that the formation of the DMPO–$O_2^{\bullet-}$ adduct is dependent on the presence of oxygen and light as well as 5,8-RS-HB. An analogous EPR spectrum is also observed when a DMSO solution of 5-RS-HB is irradiated. The addition of SOD, a specific and efficient scavenger for superoxide, should inhibit the O_2-dependent DMPO–$O_2^{\bullet-}$ adduct formation. This is observed as shown in Fig. 5. In this assay, SOD at 600 ng ml^{-1} results in a marked decrease in DMPO–$O_2^{\bullet-}$ adduct formation. SOD inhibits the EPR signal intensity. Thus, as shown in Fig. 6, the inhibition of the EPR signal intensity increases with increasing concentration of SOD. The EPR signal of the adduct is also suppressed by the addition of *p*-benzoquinone (3 mM), which is another efficient scavenger of $O_2^{\bullet-}$. We suggest that the generation of $O_2^{\bullet-}$ from 5,8-RS-HB and 5-RS-HB on photoexcitation proceeds initially via electron transfer between the excited sensitizer and its ground state to generate the semiquinone radical anion; the semiquinone radical anion then undergoes rapid re-oxidation to produce the original sensitizer and superoxide radical anion

$$5,8-RS-HB^{\bullet-} + O_2 \rightarrow 5,8-RS-HB + O_2^{\bullet-} \quad (3)$$

Electron donors which can interact with the excited state of a sensitizer can effectively switch the pathway from $^1O_2$ production to the generation of the radical anion species, which can then interact with oxygen to yield $O_2^{\bullet-}$. In addition, it is also possible for a donor, such as reduced nicotinamide adenine dinucleotide (NADH), to react directly with $^1O_2$ to produce $O_2^{\bullet-}$ [13]. However, a control experiment indicates that DEA cannot react directly with $^1O_2$ to generate $O_2^{\bullet-}$; therefore DEA was used as electron donor in our experiment. In order to confirm our inference about the formation mechanism of $O_2^{\bullet-}$, the following experiments were carried out.

1. When DEA (1 mM) is added to an O_2-saturated DMSO solution containing 5,8-RS-HB (30 μM) and DMPO (35 μM), the EPR spectrum of the DMPO–$O_2^{\bullet-}$ adduct formed is shown in Fig. 5. The addition of DEA significantly enhances the EPR signal intensity of the adduct. DEA (1 mM) results in a 15-fold enhancement in $O_2^{\bullet-}$ production. When DEA (1 mM) is added to an Ar-saturated DMSO solution containing 5,8-RS-HB (30 μM), the intensity of the 5,8-RS-HB spectrum increases by as

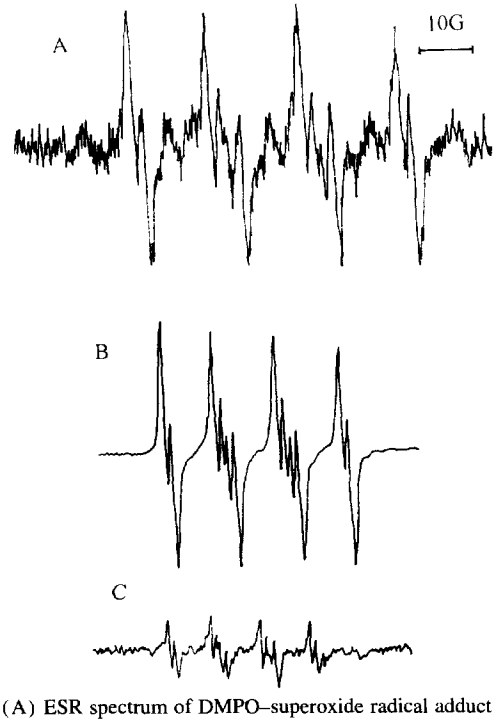

Fig. 5. (A) ESR spectrum of DMPO–superoxide radical adduct produced from the irradiation of an oxygenated DMSO solution of 5,8-RS-HB or 5-RS-HB (1 mM) and DMPO (30 mM). (B) Same as (A), but in the presence of DEA. (C) Same as (A), but in the presence of SOD. Instrumental settings: microwave power, 5.05 mW; modulation amplitude, 1.05 G; receiver gain, 2×10^5 (spectra A and C), 2×10^4 (spectrum B).

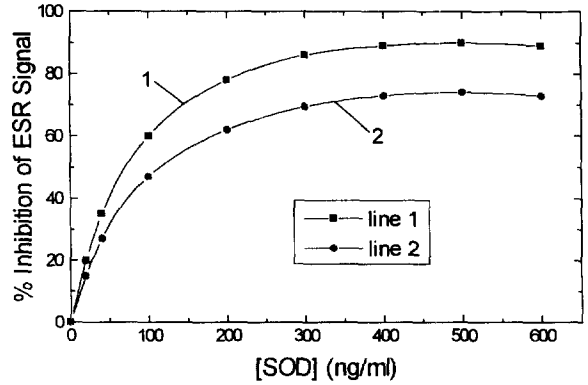

Fig. 6. Inhibition of the intensity of the DMPO–$O_2^{\bullet-}$ EPR signal by SOD. The reaction mixture, containing 5,8-RS-HB (30 μM) (line 1) or 5-RS-HB (30 μm) (line 2) and DMPO (30 mM), was irradiated in DMSO solution.

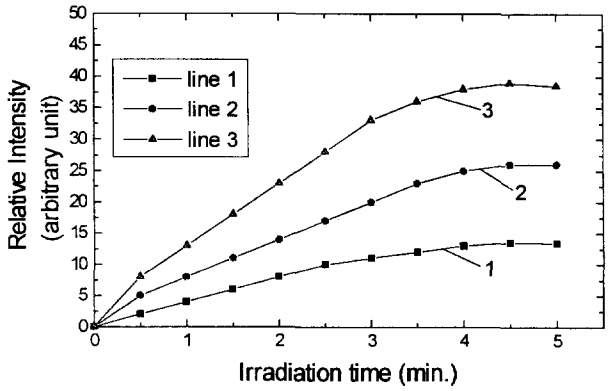

Fig. 7. Production of the spin adduct DMPO–superoxide during irradiation of oxygenated DMSO solutions of HB (0.1 mM, line 1), 5-RS-HB (0.1 mM, line 2) and 5,8-RS-HB (0.1 mM, line 3).

much as 15-fold compared with the spectrum of the sample in the absence of DEA.

2. When an Ar-saturated DMSO solution containing 5,8-RS-HB (3 μM) is illuminated with visible light, no EPR spectrum of 5,8-RS-HB$^{\bullet -}$ is observed. When the solution is bubbled with oxygen in the presence of DMPO, no EPR spectrum of the DMPO–$O_2^{\bullet -}$ adduct is detected. The two experiments indicate that the formation of the DMPO–$O_2^{\bullet -}$ adduct is dependent on the presence of semiquinone radical anion. The consistent environmental effects of the formation of $O_2^{\bullet -}$ with those of 5,8-RS-HB suggest that 5,8-RS-HB$^{\bullet -}$ is the precursor for the formation of $O_2^{\bullet -}$ by 5,8-RS-HB.

Attempts were also made to compare the $O_2^{\bullet -}$ generation abilities of 5,8-RS-HB, 5-RS-HB and HB on photosensitization. The results are shown in Fig. 7. 5,8-RS-HB can efficiently photosensitize the generation of $O_2^{\bullet -}$ and is about twofold as effective as HB. The addition of a $^1O_2$ scavenger, sodium azide, does not decrease the EPR signal intensity of the adduct, indicating that $^1O_2$ is not involved in the formation of $O_2^{\bullet -}$ by 5,8-RS-HB or 5-RS-HB to a significant extent. The negligible effect of hydrogen peroxide (5 mM) on the EPR signal of the adduct excludes the role of this species in the formation of $O_2^{\bullet -}$ by 5,8-RS-HB. Therefore the 5,8-RS-HB- and 5-RS-HB-photosensitized generation of $O_2^{\bullet -}$ in the presence of an electron donor (D) probably proceeds via Eq. (2). In the absence of the electron donor, 5,8-RS-HB$^{\bullet -}$ and 5-RS-HB$^{\bullet -}$ can be generated via Eq. (1) and then reduce O_2 to $O_2^{\bullet -}$.

3.4. Formation of hydroxyl radical

In further experiments, the production of $^{\bullet}$OH photosensitized by 5,8-RS-HB or 5-RS-HB was studied. When an oxygen-saturated DMSO–H_2O (1 : 1, v/v) solution containing 5,8-RS-HB or 5-RS-HB (30 μM) and DMPO (30 mM) is irradiated at wavelengths above 470 nm, a four-line EPR spectrum in a 1 : 2 : 2 : 1 pattern (Fig. 8(A)) is immediately observed with hyperfine coupling constants $a^N = a^H = 14.9$ G, characteristic of the hydroxyl spin adduct of DMPO (DMPO–OH). The values of the coupling constants are in good agreement with those found in the literature [14,15]. The intensity of the signal increases significantly with prolonged irradiation of the solution. Since it is known that, in aqueous solutions, DMPO–$O_2^{\bullet -}$ decomposes to form DMPO–OH, two experiments were carried out to determine whether the DMPO–OH EPR spectrum in Fig. 8 originates from DMPO–$O_2^{\bullet -}$ or from the direct addition of hydroxyl radical to DMPO. In the first experiment, an oxygen-saturated 5,8-RS-HB (30 μM) solution (DMSO–H_2O (1 : 1, v/v)) containing DMPO (30 mM) and SOD (40 μg ml^{-1}) was photoirradiated for 5 min; the production of DMPO–OH observed in the 5,8-RS-HB solution containing SOD is approximately 60% less than that obtained in an analogous experiment in the absence of SOD (Fig. 8(B)), indicating that superoxide radical anion is involved in the formation of $^{\bullet}$OH by 5,8-RS-HB or 5-RS-HB. In the second experiment, involving an oxygen-free DMSO–H_2O (1 : 1, v/v) solution of 5,8-RS-HB containing DMPO (30 mM), no EPR spectrum of DMPO–OH was observed (Fig. 8(C)). The absence of the DMPO–OH EPR spectrum indicates that the photogeneration of DMPO–OH in an air- or oxygen-saturated 5,8-RS-HB solution is oxygen dependent and is formed from DMPO–$O_2^{\bullet -}$. This result indicates that the DMPO–OH EPR spectrum observed in Fig. 8 is not generated from the direct production of hydroxyl radicals in the 5,8-RS-HB solution and their subsequent addition to DMPO, but via the decomposition of DMPO–$O_2^{\bullet -}$. In DMSO–H_2O (1 : 1, v/v) solution, the $O_2^{\bullet -}$ formed after irradiation can undergo rapid dismutation to H_2O_2 and O_2. Since transition metal ions may be present in the DMSO–H_2O solution in trace amounts, the formation of $^{\bullet}$OH in the irradiated solution of 5,8-RS-HB probably proceeds via the so-called Fenton reaction. When

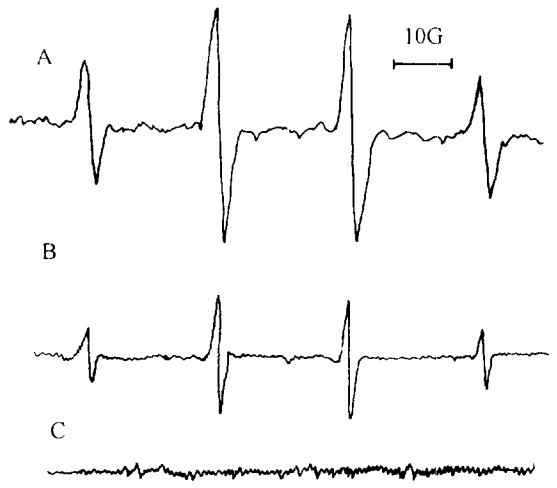

Fig. 8. (A) ESR spectrum produced from the irradiation of an oxygenated solution (DMSO–H_2O (1 : 1, v/v)) containing 5,8-RS-HB (1 mM)/5-RS-HB (1 mM) and DMPO (30 mM) above 470 nm for 2 min. (B) Same as (A), but in the presence of SOD (40 μg ml^{-1}). (C) Same as (A), but argon was bubbled through the solution. Instrumental settings: microwave power, 5.05 mW; modulation amplitude, 1.05 G; receiver gain, 2×10^4.

$FeCl_3$ is added to the solution, the DMPO–OH signal intensity is enhanced significantly.

$$O_2^{\cdot -} + H^+ \rightarrow HO_2^{\cdot} \quad (4)$$

$$H_2O + HO_2^{\cdot} + O_2^{\cdot -} \rightarrow H_2O_2 + O_2 + OH^- \quad (5)$$

$$Fe^{3+} + O_2^{\cdot -} \rightarrow Fe^{2+} + O_2 \quad (6)$$

$$Fe^{2+} + H_2O_2 \rightarrow Fe^{3+} + {}^{\cdot}OH + OH^- \quad (7)$$

Another possible pathway for the generation of $^{\cdot}OH$ may be the reaction of semiquinone radical anion with H_2O_2

$$H_2O_2 + 5,8-RS-HB^{\cdot -} \rightarrow {}^{\cdot}OH + OH^- + 5,8-RS-HB \quad (8)$$

3.5. Formation of singlet oxygen

It has been observed that $^1O_2$ is involved in many photooxygenations sensitized by perylenequinone pigments [1,2] and their complexes [16]. There are two methods available to characterize $^1O_2$: direct $^1O_2$ luminescence measurements at 1270 nm and indirect chemical trapping [17]. Diwu and Lown [8] have measured the quantum yield of $^1O_2$ generation by HA to be 0.84 (in benzene) by the 9,10-DPA photobleaching method. In order to determine the quantum yield of $^1O_2$ generation by 5,8-RS-HB and 5-RS-HB, the 9,10-DPA bleaching method was adopted and HA was used as reference. During the measurement, the absorbances at 579 nm of the samples examined were adjusted to be the same. Fig. 9 shows the rates of 9,10-DPA bleaching photosensitized by 5,8-RS-HB, 5-RS-HB and HA as a function of the irradiation time at 579 nm in $CHCl_3$. From Fig. 9, the $^1O_2$ yields for 5,8-RS-HB and 5-RS-HB in $CHCl_3$ are calculated to be 0.2 and 0.3 relative to HA (1.00). Assuming that the quantum yield of $^1O_2$ generation for HA in benzene is 0.84, the quantum yields of $^1O_2$ generation for 5,8-RS-HB and 5-RS-HB in $CHCl_3$ are estimated to be 0.17 and 0.25 respectively. However, no bleaching of 9,10-DPA was detected in the dark or in the irradiated sample without sensitizer or oxygen. These results show that singlet oxygen can be generated from 5,8-RS-HB and 5-RS-HB on photosensitization. The generation of $^1O_2$ by 5,8-RS-HB and 5-RS-HB was further confirmed by the spin trapping of TEMP, which has been proven to be an efficient $^1O_2$ acceptor.

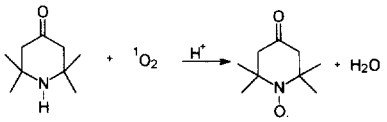

(9)

As shown in Fig. 10(B), the EPR spectrum of three equal intensity lines, characteristic of a nitroxide radical, was recorded when an oxygen-saturated solution of 5,8-RS-HB and TEMP was irradiated at room temperature. The g factor and hyperfine splitting content of the radical photogeneration by 5,8-RS-HB are identical with those of authentic TEMPO. Under similar detection conditions, irradiation of 5-RS-HB in the presence of TEMP gives an identical EPR spectrum with that of authentic TEMPO. Therefore the EPR signal obtained during irradiation of a solution containing 5,8-RS-HB or 5-RS-HB and TEMP can be attributed to TEMPO. Control experiments indicate that 5,8-RS-HB or 5-RS-HB, oxygen and light are all essential for the production of TEMPO, indicating that the formation of the nitroxide radical

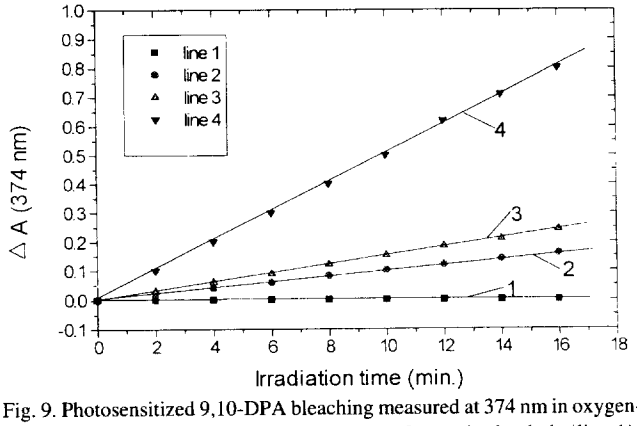

Fig. 9. Photosensitized 9,10-DPA bleaching measured at 374 nm in oxygen-saturated $CHCl_3$ with no sensitizer or oxygen-free or in the dark (line 1), with 5,8-RS-HB (line 2), with 5-RS-HB (line 3) and with HA (line 4) (in benzene) as a function of the irradiation time.

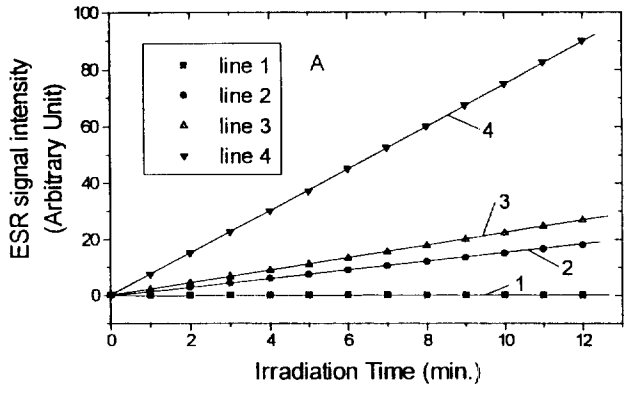

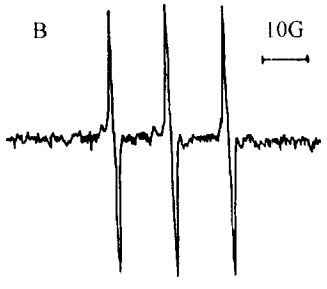

Fig. 10. (A) Formation of TEMPO during the illumination of solutions containing different sensitizers in the presence of TEMP at room temperature in $CHCl_3$. With no sensitizer or oxygen-free or in the dark (line 1), with 5,8-RS-HB (line 2), with 5-RS-HB (line 3) and with HA (line 4). (B) ESR spectrum produced by irradiation of an oxygenated solution containing 5,8-RS-HB or 5-RS-HB (0.1 mM) and TEMP (15 mM). Instrumental settings: microwave power, 5.05 mW; modulation amplitude, 1.05 G; receiver gain, 2×10^4.

is a photodynamic process. Comparative studies between 5,8-RS-HB, 5-RS-HB and HA indicate that 5,8-RS-HB and 5-RS-HB can also generate $^1O_2$. It can be calculated from Fig. 10 using HA as reference that the quantum yields of generation of $^1O_2$ by 5,8-RS-HB and 5-RS-HB are the same as in 9,10-DPA bleaching experiments in $CHCl_3$. Thus the results obtained from EPR and the 9,10-DPA bleaching methods are consistent.

In order to investigate further the role of singlet oxygen in the formation of TEMPO radical from TEMP, the effect of deuterium on the yield of TEMPO was studied during the photoirradiation of 5,8-RS-HB or 5-RS-HB in $CHCl_3$. When samples containing 5,8-RS-HB or 5-RS-HB (30 μM) and TEMP (50 μM) were irradiated separately in oxygen-saturated solutions of $CHCl_3$ and $CDCl_3$, the EPR signal intensities of the TEMPO radical were threefold larger in $CDCl_3$ than in $CHCl_3$. Since the lifetime of singlet oxygen is 10–15 times longer in deuterated solvents than hydrated solvents, the increased TEMPO accumulation in deuterated solvents is anticipated. These results further support the contention that the photoirradiation of 5,8-RS-HB or 5-RS-HB generates singlet oxygen which, in turn, reacts with TEMP to form TEMPO radical.

The EPR signal was suppressed by $^1O_2$ scavengers such as azide and tetramethylethylene. Sodium azide is commonly used to inhibit oxygen-dependent reactions. In order to estimate the quenching rate constant of sodium azide, different concentrations of sodium azide were used to establish a competition reaction between NaN_3 and TEMP for the available $^1O_2$. Fig. 11 shows a Stern–Volmer plot of the effect of NaN_3. The Stern–Volmer behaviour of NaN_3 quenching is linear up to at least 2 mM NaN_3. The bimolecular quenching rate constant for NaN_3 was estimated according to dynamic quenching, where k_T is the rate for TEMP, k_d is the decay rate and k_q is the rate for sodium azide. From this, it follows that

$$\phi_{TEMPO} = \frac{k_T[T]}{k_T[T] + k_d + k_q[Q]} \quad (10)$$

$$\frac{\phi_0}{\phi} = \frac{k_T[T] + k_d + k_q[Q]}{k_T[T] + k_d} = 1 + \frac{k_q}{k_T[T] + k_d}[Q] \quad (11)$$

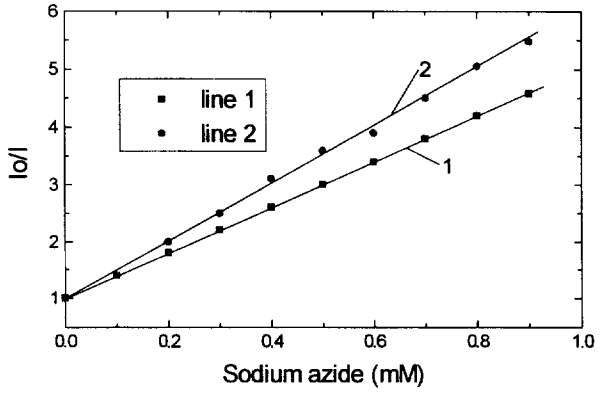

Fig. 11. Stern–Volmer quenching of the EPR signal intensity of TEMPO by NaN_3, performed by adding various amounts of NaN_3 to a series of oxygen-saturated $CHCl_3$ solutions containing 5,8-RS-HB (line 1) or 5-RS-HB (line 2) (0.2 mM) and TEMP (15 mM).

According to this equation, the bimolecular constants of 5,8-RS-HB and 5-RS-HB for NaN_3 quenching were calculated to be 2.65×10^8 M^{-1} s^{-1} and 3.13×10^8 M^{-1} s^{-1} respectively using $k_t = 4 \times 10^7$ M^{-1} s^{-1} determined by Lion et al. [18] for a related amine and 160 μs for $^1O_2$ in $CHCl_3$ [19]. The above results suggest that TEMPO is derived from the reaction of TEMP with $^1O_2$ generated by the irradiation of 5,8-RS-HB or 5-RS-HB shown in Eq. (9).

3.6. Transformation between 5,8-RS-HB or 5-RS-HB semiquinone anion and activated oxygen species and the effect of oxygen on the competition between type I and type II mechanisms of 5,8-RS-HB/5-RS-HB photosensitization

The formation of 5,8-RS-$HB^{\bullet -}$, 5-RS-$HB^{\bullet -}$, $^1O_2$, $O_2^{\bullet -}$ and $^{\bullet}OH$ depends on oxygen, which can be reduced by 5,8-RS-$HB^{\bullet -}$ or 5-RS-$HB^{\bullet -}$ to give $O_2^{\bullet -}$. Oxygen plays a key role in the transformation between 5,8-RS-$HB^{\bullet -}$, 5-RS-$HB^{\bullet -}$, $^1O_2$, $O_2^{\bullet -}$ and $^{\bullet}OH$. It was therefore of interest to investigate the effect of the oxygen concentration on the formation of 5,8-RS-$HB^{\bullet -}$/5-RS-$HB^{\bullet -}$, $^1O_2$ and $O_2^{\bullet -}$.

The unique dual role of TEMPO, applicable for both the detection of $^1O_2$ and 5,8-RS-$HB^{\bullet -}$/5-RS-$HB^{\bullet -}$, can be conveniently taken advantage of following the transformation between 5,8-RS-$HB^{\bullet -}$/5-RS-$HB^{\bullet -}$/$HB^{\bullet -}$ and $^1O_2$ as the oxygen concentration changes. As shown in Fig. 12, in the sealed system of 5,8-RS-HB/5-RS-HB/HB and TEMP, saturated by oxygen prior to illumination, the EPR intensity of TEMPO increases up to a maximum within 8 min, 12 min and 15 min for 5,8-RS-HB, 5-RS-HB and HB respectively, and then decreases as the irradiation proceeds. The TEMPO-increasing process is caused by the reaction of TEMP with $^1O_2$ as shown in Eq. (9), and the TEMPO-decreasing process results from the spin destruction of TEMPO by 5,8-RS-HB/5-RS-HB/HB semiquinone radical as shown below

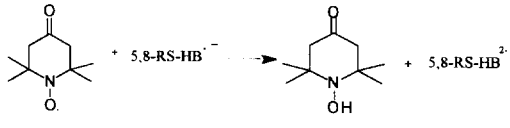

(12)

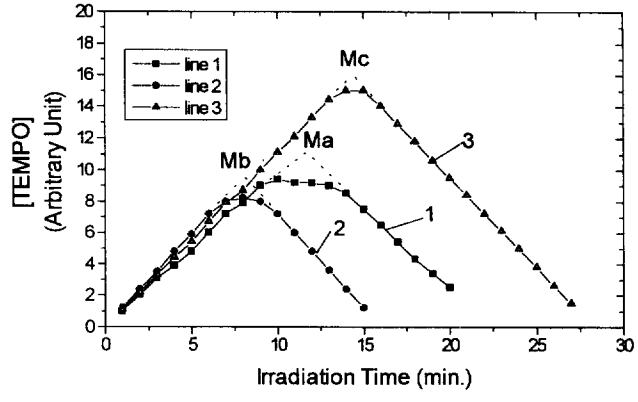

Fig. 12. Dependence of the competition between 5-RS-HB (line 1), 5,8-RS-HB (line 2) or HB (line 3) semiquinone radical and singlet oxygen on the oxygen concentration of a sealed system during irradiation in DMSO. Plot of the concentration of TEMPO as a function of irradiation time.

The decreasing oxygen concentration of the sealed system caused by Eq. (3) suppresses the formation of $^1O_2$, but promotes the generation of 5,8-RS-HB$^{\bullet -}$/5-RS-HB$^{\bullet -}$. Fig. 12 shows the turning points Ma/Mb/Mc, where the accumulation of $^1O_2$ is replaced by that of 5,8-RS-HB$^{\bullet -}$/5-RS-HB$^{\bullet -}$/HB$^{\bullet -}$ when the oxygen in the system is consumed completely, indicating that oxygen plays a critical role in the competition between type I and type II mechanisms of 5,8-RS-HB and 5-RS-HB photosensitization.

4. Conclusions

Both electron transfer (type I) and $^1O_2$ (type II) paths are involved in 5,8-RS-HB and 5-RS-HB photosensitization to different extents, depending on the oxygen and 5,8-RS-HB/5-RS-HB concentrations and environmental factors, such as the nature of the substrate coexisting with the sample. In a hypoxic medium, the semiquinone radical, arising from a type I mechanism, is primarily responsible for 5,8-RS-HB/5-RS-HB photosensitization. In oxygenated medium, the 5,8-RS-HB/5-RS-HB photosensitization is largely mediated by $O_2^{\bullet -}$, but the supplemental role of $^1O_2$ and $^{\bullet}OH$ should also be considered.

Acknowledgements

This research was supported by the National Science Foundation of China (No. 59473023).

References

[1] L.J. Jiang, The structures, properties, photochemical reaction and reaction mechanisms of hypocrellins (I), Kexue Tongbao 21 (1990) 1608–1616.
[2] L.J. Jiang, The structures, properties, photochemical reactions and reaction mechanisms of hypocrellins (II), Kexue Tongbao 22 (1990) 1681–1690.
[3] Z.J. Diwu, J.W. Lown, Hypocrellins and their use in photosensitization, Photochem. Photobiol. 52 (1990) 609–616.
[4] N.W. Fu, Y.X. Chu, J.Y. An, Photodynamic action of hypocrellin A on hepatoma cell mitochondria and microsomes, Acta Pharm. Sin. 10 (4) (1989) 371–373.
[5] J.B. Wang, J.N. Bao, Clinical analysis and observation of hypocrellin photochemistry in treatment of lichen amyloidosis in 37 patients, J. Chin. Acad. Med. 7 (5) (1985) 349–351.
[6] R.Y. Liang, G.D. Mei, W.Y. Zhou, 62 cases with hypertrophic scars treated with hypocrellin photochemotherapy, Chin. J. Denna 15 (1982) 87–88.
[7] L.Y. Zang, Z.Y. Zhang, H.P. Misra, EPR studies of trapped singlet oxygen ($^1O_2$) generated during photoirradiation of hypocrellin A, Photochem. Photobiol. 52 (1990) 677–683.
[8] Z.J. Diwu, J.W. Lown, Photosensitization by anticancer agents 12. Perylene quinonoid pigments, a novel type of singlet oxygen sensitizer, J. Photochem. Photobiol. A: Chem. 64 (1992) 273–287.
[9] Y.Z. Hu, J.Y. An, L.J. Jiang, Studies of the sulfonation of hypocrellin A and the photodynamic actions of the product, J. Photochem. Photobiol. B: Biol. 17 (1993) 195–201.
[10] J. Mayer, R. Krasluklanis, Absorption spectra of the radical ions of quinones: a pulse radiolysis study, J. Chem. Soc., Faraday Trans. 87 (1991) 2943–2947.
[11] Z.J. Diwu, C.L. Zhang, J.W. Lown, Photosensitization with anticancer agents. 18. Perylenequinonoid pigments as potential photodynamic therapeutic agents: preparation and photodynamic properties of amino-substituted hypocrellin derivatives, Anti-Cancer Drug Design 8 (1993) 129–143.
[12] J.R. Harbour, M.L. Hair, Detection of superoxide ions in nonaqueous media. Generation by photolysis of pigment dispersions, J. Phys. Chem. 82 (12) (1978) 1397–1399.
[13] G. Petters, M.A.J. Rodgers, Singlet electron transfer from NADH analogues to singlet oxygen, Biochim. Biophys. Acta 637 (1981) 43–52.
[14] E. Finkelstein, E.G.M. Rosen, E.J. Rauckman, Spin trapping. Kinetics of the reaction of superoxide and hydroxyl radicals with nitrones, J. Am. Chem. Soc. 102 (1980) 4994–4999.
[15] K. Lang, M. Wagnerova, P. Stopka, W. Dameran, Reduction of dioxygen to superoxide photosensitized by anthraquinone-2-sulphonate, J. Photochem. Photobiol. A: Chem. 67 (1992) 187–195.
[16] Z.J. Diwu, C.L. Zhang, J.W. Lown, Photosensitization of anticancer agents 13. The production of singlet oxygen by halogenated and metal-ion-chelated perylenequinones, J. Photochem. Photobiol. A: Chem. 66 (1992) 99–112.
[17] C.S. Foote, in A. Quintanilha (Ed.), Reactive Oxygen Species in Chemistry, Biology and Medicine, Plenum, New York, 1988, pp. 97–116.
[18] Y. Lion, E. Gandin, A. van de Vorst, On the production of nitroxide radicals by singlet oxygen reaction: an EPR study, Photochem. Photobiol. 31 (1980) 305–309.
[19] T.A. Jenny, N.J. Turro, Solvent deuterium isotope effects on the lifetime of singlet oxygen determined by direct emission spectroscopy at 1.27 μm, Tetrahedron Lett. 23 (1982) 2923.